RSC Advances

ROYAL SOCIETY OF CHEMISTRY

www.rsc.org/advances

Table of contents entry: Molybdovanadophosphate-based surfactant encapsulated heteropolyanion with multi-lamellar nano-structure for ambient condition catalytic wet air oxidation of BPA.

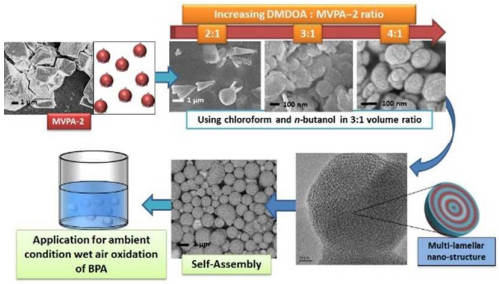

Journal Name

ARTICLE

A molybdovanadophosphate-based surfactant encapsulated heteropolyanion with multi-lamellar nano-structure for catalytic wet air oxidation of organic pollutant under ambient conditions

Received 00th January 20xx,
Accepted 00th January 20xx

DOI: 10.1039/x0xx00000x

www.rsc.org/

Shun Kuang Lua,[a,b,c] Wen-Da Oh,[a,b,d] Li-Zhi Zhang,[b] Lei Yao,[b,c] Teik-Thye Lim[d] and ZhiLi Dong*[c]

A series of surfactant encapsulated heteropolyanion (SEH-n) based on molybdovanadophosphates (MVPs) was prepared. The morphological optimisation of the SEHs was studied by the control of solvent polarity and MVP to surfactant ratio used. Investigation by TEM revealed the formation of particles with multi-lamellar nano-structure in the SEHs. Characterization of the SEHs by XRD, TGA and FTIR indicated the successful encapsulation of the molybdovanadophosphates with the surfactant. The performance of SEHs as catalysts for the removal of bisphenol–A under ambient conditions was evaluated. Factors influencing the performance of the SEH–n are the relative stability of the Keggin structure and electron accepting property. The dissolved oxygen plays a crucial role in improving the BPA removal efficiency. The hydrophobic property of the nano–sized SEHs provides good aqueous stability and allows excellent recoverability of the catalyst from the aqueous solution after treatment.

1. Introduction

The design and development of advanced functional materials is an area of growing interest in the last few decades. Such research will bring the advancement to the applications of these materials in material science and catalysis.[1] One of the key steps towards the realization of this development is the controlled self-assembly of nano-building blocks into functional assemblies which is technically challenging.[2] Polyoxometalates (POMs) is a type of molecular transition metal oxide gaining research interest in the preparation of advanced functional assemblies. They are oxoanionic cluster made up of early transition metals in their highest oxidation state i.e. tungsten, molybdenum and vanadium. POMs have attracted much research interest and have been applied in areas such as materials, catalysis, biomedicine, energy and environmental studies.[3-7] Amongst the chemical and physical properties of POMs, the redox and semiconductor like properties[8] are some of the main driving forces for the active research on this material. The use of POM in both aqueous and organic media under homogeneous condition for fine organic synthesis[9-11] and their potential in the mineralization of organic compounds are well-documented.[12-14] However, homogeneous catalysis using POM is an obstacle to effective application difficulty due to difficulty in catalyst recovery.

The most commonly studied POM is the heteropolyacid (HPA) best represented by the Keggin structure. HPA typically have low surface area and high solubility in water which hinders the recoverability and effective use as catalytic materials in aqueous media.[15] A strategy to achieve heterogeneity of the HPAs and facilitate their recoverability from aqueous solution is the substitution of the acidic protons with large inorganic countercations (e.g. Cs^+). Another method employs organic cations to form organic–inorganic hybrids presents a solution to obtain interesting functional nano-structures of POM. Such hybrid basing on electrostatic interaction presents a facile method of synthesis in addition to other merits of improving catalyst recoverability and reusability. Surfactant encapsulation is an emerging methodology to synthesize self-assembled POMs nano-architectures. The use of quaternary ammonium surfactants like dimethyldioctadecylammonium (DMDOA) with good stability and twin alkyl chains can provide platform for morphological control.

To date, several examples of surfactant encapsulated POMs with various architectures such as disk, cone, and flower have been reported.[16, 17] While much work and development has been achieved on the aspects of structural and morphological studies,[18, 19] works reporting the application of POMs architectures in advanced oxidation processes are limited. The synthesis of POMs with nano–architectures remains a daunting task due to the high crystalline energy and hydrophilic nature of POMs clusters.[1] This makes self-assembly nano-architecture of POMs a field of research worth exploring.

[a] Interdisciplinary Graduate School, Nanyang Technological University, 50 Nanyang Avenue, Singapore 639798, Singapore.
[b] Nanyang Environment and Water Research Institute,Nanyang Technological University, 1 Cleantech Loop, CleanTech One, Singapore 637141, Singapore.
[c] School of Materials Science and Engineering, Nanyang Technological University, 50 Nanyang Avenue, Singapore 639798, Singapore. Email: zldong@ntu.edu.sg; Fax: +65-6791 9081; Tel: +65-6790 6727
[d] Division of Environmental and Water Resources Engineering, School of Civil and Environmental Engineering, Nanyang Technological University, 50 Nanyang Avenue, Singapore 639798, Singapore

Among the various structural variations of POMs, the Keggin structure is one of the most investigated as compared to the other members of the HPA family. The $H_{3+n}[PMo_{12-n}V_nO_{40}]$ series of mixed addenda Keggin type heteropolyanion has found wide applications in the selective oxidation for organic synthesis and other areas.[20-23] The preference can be mainly associated to their high redox reversibility in which re-oxidation can be achieved with molecular oxygen as a benign oxidant,[20] making them attractive oxidation catalysts and thus their viability to be developed as advanced functional materials.

In this study HPA of the series $H_{n+3}[PMo_{(12-n)}V_nO_{40}]$ (n = 1, 2, 3), herein denoted as MVPA–1, MVPA–2 and MVPA–3 were prepared. The MVPAs were then modified by a simple cationic exchange reaction with a quaternary ammonium surfactant, dimethyldioctadecylammonium bromide (DMDOA·Br), to give a series of surfactant encapsulated heteropolyanions (SEH–n) The as-prepared SEH–n are self-assembled inorganic-organic hybrid material with defined spherical morphology and multi-lamellar nano-structure (MLNS), the tuneable nature of the anions allows the optimisation of the catalyst for catalytic wet air oxidation of organic pollutant under ambient conditions. The research and translation of HPA into effective catalyst for application in environmental remediation is crucial in the development as an effective molecular catalyst. Contrary to typical catalytic wet air oxidation (CWAO) process which requires high temperature and pressure[24], CWAO using these SEHs demonstrating MLNS were capable of the removal of a recalcitrant organic pollutant, bisphenol A (BPA) from water under ambient conditions. The current work is essential in the understanding of (i) the formation and structural characteristics of the amphiphilic catalyst, and (ii) the feasibility of their application towards environmental remediation which requires less energy and chemical usage in water treatment processes.

2. Experimental

2.1. Chemicals

Na_2HPO_4, $NaVO_3$, $Na_2MoO_4{\cdot}2H_2O$, $(C_{18}H_{37})_2(CH_3)_2NBr$, bisphenol A (BPA) and $CHCl_3$ were purchased from Sigma-Aldrich and used without further purification. Sulfuric acid (95 – 97%) and diethyl ether were purchased from Honeywell and Fischer Scientific respectively. All solutions were prepared using MilliQ (MQ) water (18.2 MΩ cm^{-1}) unless otherwise stated. Molybdovanadophosphoric acid (MVPA-n) of the series $H_{3+n}(PMo_{12-n}V_nO_{40})$ (n = 1, 2, 3) were prepared as reported elsewhere[25] and was recrystallized from solution for further synthetic modification.

2.2. Synthesis and preparation of materials

The synthesis of the surfactant encapsulated heteropolyanions (SEHs) uses a single phase approach.[26] In the particular synthesis of SEH–1 $((C_{18}H_{37})_2(CH_3)_2N)_4[PMo_{11}VO_{40}]$, the surfactant, dimethyldioctadecylammonium bromide (DMDOA·Br) (2.83g, 4.48 mmol) was firstly dissolved into a solvent mixture of n-butanol and chloroform in 1:3 volume ratio. The solid MVPA–1 (2.0 g, 1.12 mmol) is added in small portions with ultra-sonication to ensure that each portion is fully dissolved and a clear solution is obtained after each addition. This is performed such that the ratio of MVPA to surfactant was slowly adjusted to 1:4. After the complete addition of MVPA–1, the solvent was allowed to evaporate to dryness and the solid material was collected, herein denoted as surfactant encapsulated heteropolyanion–1 (SEH–1). The same procedure was followed using MVPA–2 and MVPA–3 with adjustment in the stoichiometric ratio of surfactant added, where SEH–2 and SEH–3 were collected upon evaporation of solvent.

2.3. Material characterization

The morphological transformation of the MVPA to SEH was examined using a field emission scanning electron microscope (FESEM JEOL-7600F), the local structure of the SEHs was studied using high resolution transmission electron microscope (HRTEM) (TEM JEOL-2100F) microscope with an acceleration voltage of 200 kV. Powder samples were loaded onto a PMMA sample holder and X-ray diffraction (XRD) patterns were obtained by Bruker D8 Advance X-ray diffractometer with monochromated CuKα radiation (λ = 1.5418 Å) in 2θ range of 5 – 50° with step size of 0.02°/s. The Brunauer-Emmett-Teller (BET) surface area was determined using N_2 adsorption-desorption isotherm analysis at 77 K (Quantachrome Quadrasorb SI). The Fourier transform infrared (FTIR) spectroscopy of the samples was performed using Perkin Elmer GX over the range of 4000 – 400 cm^{-1}. Thermo-gravimetric analysis of the materials was carried out using TA Instruments Q500 under nitrogen flow of 40 mL min^{-1} and a heating rate of 10°C min^{-1}.

2.4. Catalytic Performance Studies

In the catalytic oxidation experiment using the SEHs, 1.0 g L^{-1} loading of SEH–n was added into an aqueous solution of bisphenol-A (BPA) (20 mg L^{-1}, 50 mL) at the natural pH of the solution under ambient conditions. The reaction vessel was covered during the oxidation experiment to preclude any interaction with light and reduce the loss of water. The reaction was deemed to have started upon the addition of the SEHs, which excludes any time for the attainment of adsorption–desorption equilibrium. Air was bubbled through the solution at a rate of 3.5 L min^{-1} through the solution for provision of dissolved oxygen as the oxidant for the catalytic wet air oxidation. Samples were drawn from the reactor at fixed time intervals and tested for BPA concentration in the solution using a Hypersil Gold reversed phase column (Thermo Scientific) with mobile phase composition of 60% acetonitrile and 40% deionized water at a flow rate of 1 mL min^{-1} on a Perkin Elmer HPLC system equipped with a UV-vis detector operating at 220 nm. The solutions were analysed after reaction with inductive coupled plasma–optical emission spectrometer for dissolved metals (ICP-OES, Perkin

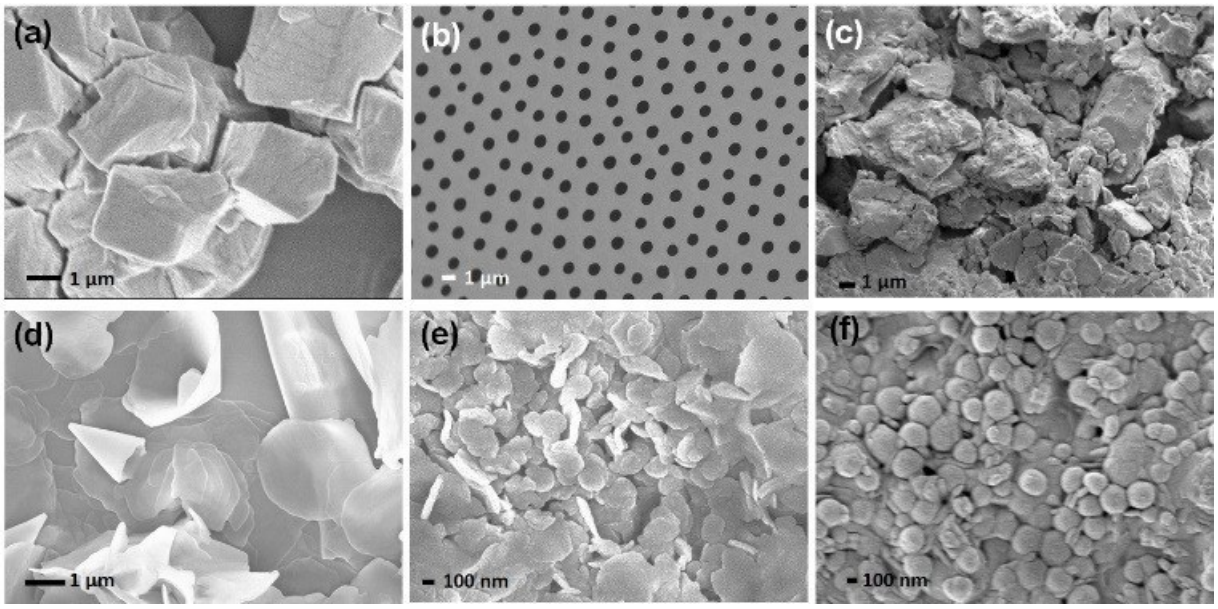

Fig. 1. SEM micrograph of (a) MVPA–2, (b) casted film of SEH, (c) bulk powder of SEH, (d) MVPA-2: DMDOA in ~1:2 ratio, (e) MVPA-2:DMDOA in ~1:3 ratio and (f) SEH from mixed solvent of chloroform : n-butanol in 3:1 ratio.

Elmer Optima 2000DV). XPS analysis was performed using JPS-9030 Photoelectron Spectrometer (JEOL, Japan) using non-monochromatic Mg K_α X-ray source with pass energy of 50 eV and analysis area of ~3 mmϕ.

3. Results and discussion

3.1. Materials Characterization

Fig. 1(a) shows the FESEM micrograph of MVPA–2. The MVPAs are generally water-soluble crystalline solids preventing their effective recovery from aqueous system. In this regards, the heterogeneity was introduced by replacing the exterior protons of MVP with DMDOA. The DMDOA was introduced via a simple cation modification method. After modification, the MVPs encapsulated in the SEHs are active sites supported with a surfactant matrix allow them to be effectively stabilised and used as a catalyst. The morphological transformation effect of the surfactant to MVP ratio on the series of Keggin HPA is studied using FESEM by following the transformation of the SEH from the HPA precursor at different surfactant to MVP ratios.

The preparation of SEHs with pure chloroform as the solvent via synthesis route 1 (Fig. 2) leads to the formation of a porous membrane-like structure with pores of 1 μm in diameter (Fig. 1(b)). Bulk SEH pulverized into fine powdered material does not allow us to obtain small particles with any controllable morphology as can be seen in Fig. 1(c). Therefore the introduction of a co-solvent such as *n*-butanol is required to adjust the solvent polarity for morphological control of the SEHs. Since all MVP have similar diameter of *ca.* 1 nm, the directing force for controlled morphology will come from (i) solvent polarity control and (ii) stoichiometry control of the surfactant used. The formation of SEH particles with narrower size distribution is obtained by adding *n*-butanol as a stabilizer during SEH synthesis[16] and solvent evaporation under ambient conditions can be achieved. With the addition of n-butanol to chloroform at volume ratio of 1:3 in synthesis route 2 (Fig. 2), we explore the effect of DMDOA to MVPA at different ratios on the SEH synthesis. Fig. 1(d) shows that with a ratio of approximately 2 DMDOA: 1 MVPA, mixed morphologies of nano-disk and nano-cone are obtained. Fig. 1(e) shows that the addition of DMDOA up to a ratio of 3:1 leads to the evolution of spherical particles with 150–200 nm in diameter. When stoichiometric amounts of DMDOA is added to the respective MVPA (i.e. MVPA–1: 4:1, MVPA–2: 5:1 and MVPA–3: 6:1) to replace all the protons, spherical particles starts to evolve as evidently shown in Fig 1(f). Considering that the Keggin-type POMs has a radius of 0.52 nm,[27] the surface area of a single MVP anion is estimated to be around 3.42 nm^2. The lateral area (0.567 nm^2) per DMDOA[28] therefore fully occupy the surface of MVPA–3, restricting the freedom of spatial arrangement with increase of DMDOA on the series of MVPA. As such, the complete substitution of the protons by DMDOA with the control of the solvent polarity exclusively leads to the formation of spherical particles. Therefore, the increment of anionic charge on the MVPAs from −4 to −6 has no significant influence on the morphology. A mixed solvent system consisting of $CHCl_3$ and *n*-butanol (as the co-solvent) at the ratio of 1:3 was thus employed as the optimum synthesis condition to obtain spherical SEHs. In order to establish an equal platform for the catalytic studies, with primary focus on the activity of molybdovanadophosphates (MVP) (i.e. based on the degree of vanadium substitution), it is preferable that all the SEHs have a similar morphology.

We propose that formation of the primary building blocks (i.e. $(DMDOA_4(PMo_{11}VO_{40}))$ by the complete replacement of the H^+ in the MVPAs with the DMDOA surfactant is essential for the formation of spherical architecture. This is shown by the changes in the morphology of the SEH with increase in

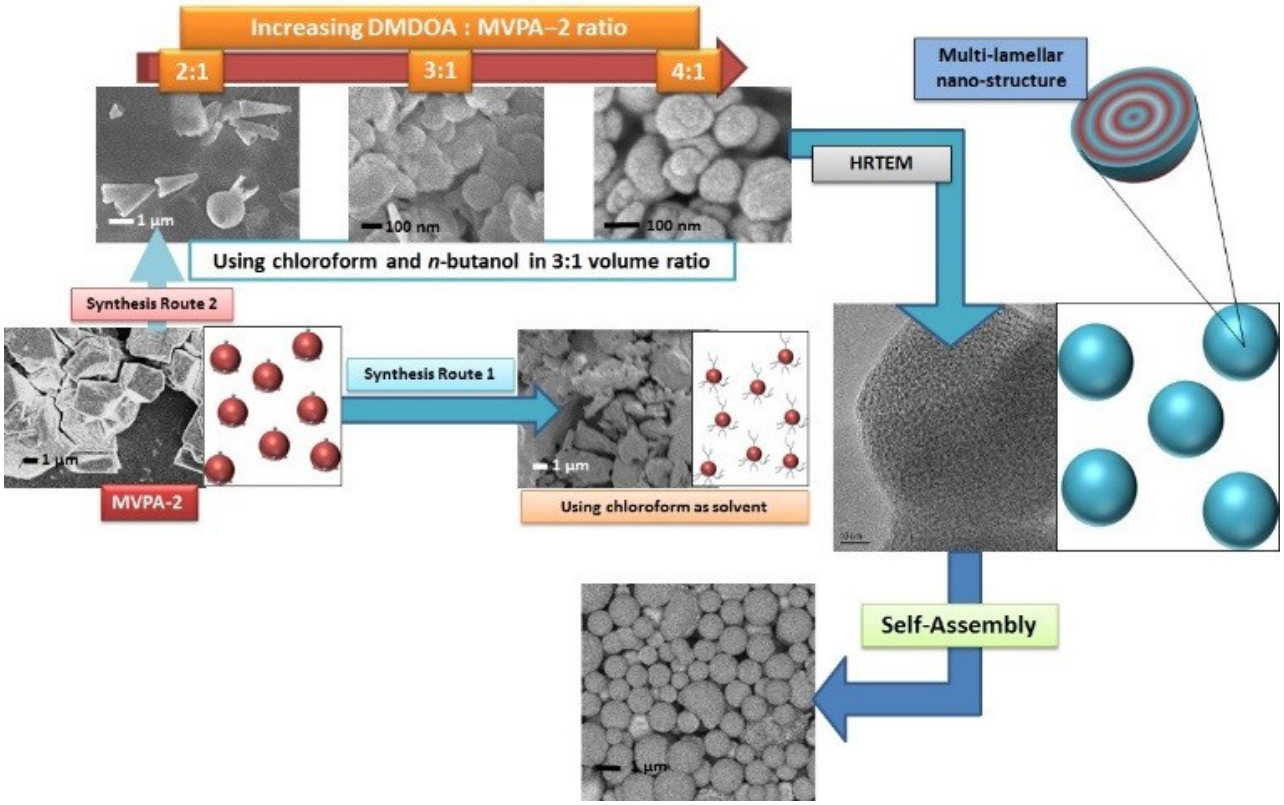

Fig. 2. Schematic illustration for synthesis and formation of SEH-2 from MVPA-2 and influence of DMDOA:HPA ratio.

surfactant added as shown in Fig. 2. Only with the formation of the required primary building blocks, the self-assembly process to form a secondary spherical architecture with MLNS can be attained.

As shown by the HRTEM micrographs in Fig. 3, all the SEHs have spherical architecture with nano-dimensional MLNS. Due to the presence of molybdenum which reduces the transmission of electrons through the specimen, the MLNS is generally obscured in SEHs of larger sizes. Identifying a smaller particle in the micrograph of SEH–3 (Fig. 3(c)) allows us to effectively observe the presence of the MLNS with an interlayer distance of approximately 1.5 nm. This cluster self-assembly is typical of twin alkyl chain surfactants which forms vesicles with MLNS in solutions. While the lighter region consists of the surfactants, the darker regions consisting of nano-sized cluster *ca.* 1 nm in size (Fig. 3(d)) which shows the presence of Keggin anions within the SEH. The structural integrity of the Keggin anions is deemed to be retained throughout the modification process and is effectively stabilized within the surfactant encapsulation.

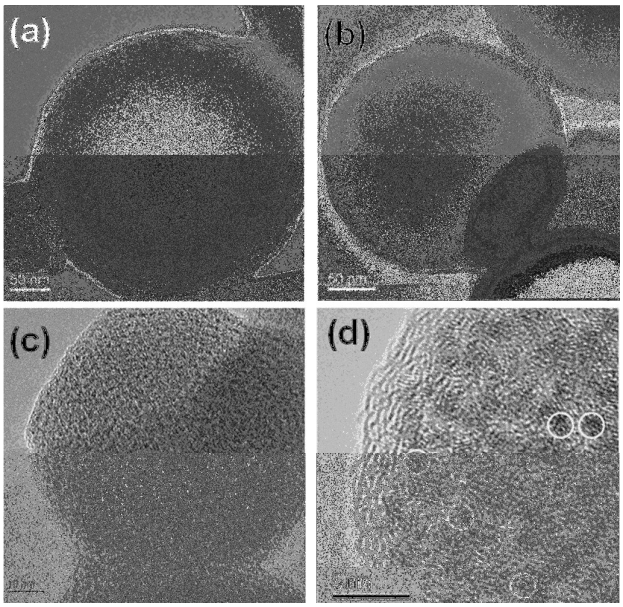

Fig. 3. High-resolution TEM micrograph of (a) SEH–1, (b) SEH–2, (c) SEH–3 and (d) SEH–2 at showing lattice fringes about 0.2 nm d-spacing inside each Keggin cluster with a diameter of ca. 1 nm (white circles).

Fig. 4 shows the XRD patterns of MVPA–1, DMDOA·Br and SEHs. The series of MVPAs prepared has a tetragonal crystal structure with space-group P4/mnc. As the increment in the substitution of Mo by V has little effect on the crystallographic arrangement of the material, XRD pattern of MVPA–1 presented here is representative of the MVPAs prepared. The EDX analysis performed on the MVPAs shows that the atomic percentage of phosphorus, molybdenum and vanadium estimated from the analysis matches the theoretical percentage (Table 1). All the reflections can be indexed to be coming from the single phase $H_4PMo_{11}VO_{40} \cdot 32\ H_2O$ (PDF#00-045-0611), which shows the MVPAs are prepared successfully. After modification with DMDOA, the typical reflection peaks of

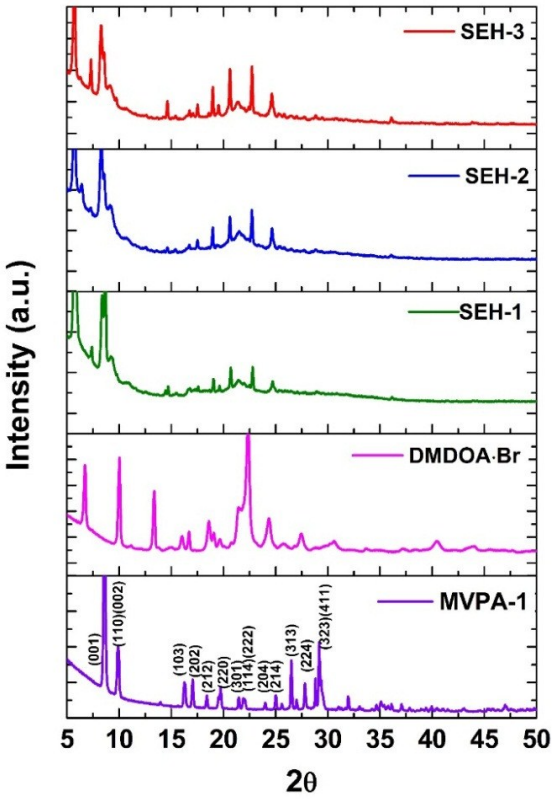

Figure 4. XRD patterns of MVPA-1, DMDOA·Br, SEH-1, SEH-2 and SEH-3. The peaks of MVPA-1 is indexed to single phase $H_4PVMo_{11}O_{40}$. Peaks in all SEHs between 15-25° indicates the presence of MLNS.

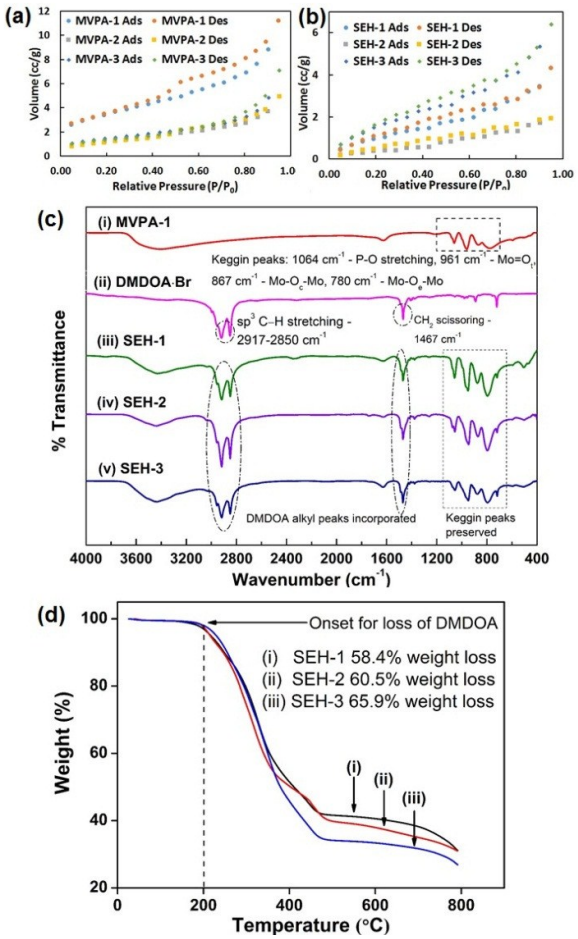

Fig. 5. BET sorption isotherm of (a) MVPAs and (b) SEHs. (c) FTIR of (i) $H_4[PMo_{11}VO_{40}]$, (ii) dimethyldioctadecylammonium bromide (iii) SEH–1, (iv) SEH–2 (v) SEH–3. (d)Thermo-gravimetric analysis weight loss profile of (i) SEH–1 (ii) SEH–2 (iii) SEH–3

MVPA crystalline structure is no longer observed. The replacement of the protons by DMDOA and the loss of water of crystallization transformed the structure of the resulting SEHs. This leads to the transition from a crystalline solid to an amorphous material with MLNS. The observed reflections at *ca.* 5.7° and 8.3° are higher order reflections from the basal layer spacing in the MLNS. The Bragg reflection at 5.7° corresponds to the spacing of 1.6 nm which is in close agreement with the observed lamellar spacing in the HRTEM micrograph. The observed spacing suggests that the alkyl chains of the DMDOA are almost fully interdigitated which confines them to a tight and rigid structure. This results in the XRD peaks in typical Keggin anions in the range of 15–30° to be convoluted after modification with DMDOA. The new Bragg reflections arising between 15–25° are indicators of the rigid structure formed by the alkyl chains of DMDOA in the lamellar nano-structure as it becomes the determining factor in morphological control and the structure of the SEHs.

The EDX analysis performed on the SEHs shows that while phosphorus is undetectable due to the encapsulating matrix, the molybdenum to vanadium ratio estimated from analysis is in good agreement with theoretical percentage (Table 1). Fig 5(a) and (b) shows the BET sorption isotherm of the MVPAs and SEHs with their associated values as summarised in table 1. While the surfactant modifies the SEH into a heterogeneous catalyst, it is interesting to note that the specific surface was not enhanced as a result of the modification. The SEH has a

Table 1. EDX analysis providing semi-quantitative results of phosphorus, molybdenum and vanadium in MVPAs and SEHs normalized to 100% and BET surface area of MVPAs and SEHs. Phosphorus is not detectable by EDX in all SEH.

	Atomic % P		Atomic % Mo		Atomic % V		
	Theoretical	Experimental	Theoretical	Experimental	Theoretical	Experimental	BET surface area/ $m^2 g^{-1}$
MVPA–1	7.7	7.5	84.6	83.0	7.7	9.5	12.1
MVPA–2	7.7	7.6	76.9	75.0	15.4	17.3	4.4
MVPA–3	7.7	7.3	69.2	69.5	23.1	23.2	5.2
SEH–1	-	-	91.7	90.1	8.3	9.9	4.3
SEH–2	-	-	83.3	85.1	16.7	14.9	1.5
SEH–3	-	-	75.0	74.6	25.0	25.4	6.9

closely-packed MLNS, which results in low pore volume and porosity. Therefore the surface area is largely limited to the external surface, leading to the SEHs having low specific surface area.

Fig. 5(c) shows the FTIR spectra. Characteristic peaks of the Keggin anion structure at 1064, 961, 867 and 780 cm^{-1} (Fig. 5(i)) corresponding to P–O stretching, Mo=O_t stretching of terminal oxygen, Mo–O_c–Mo stretching of corner-sharing MoO_6 octahedra and the edge sharing MoO_6 octahedra of Mo–O_e-Mo respectively is observed in MVPA–1. In the SEHs, the peaks are slightly shifted, i.e. in SEH–1, the characteristic peaks of Keggin anions are now at ~1060 cm^{-1}, 953 cm^{-1}, 877 cm^{-1} and 796 cm^{-1}. Additional bands are also observed for all the SEHs at 2917–2850 cm^{-1} and 1467 cm^{-1} attributed to the alkyl chain sp^3 C–H stretching and CH_2 scissoring of the quaternary amine surfactant DMDOA (Figure 5(c) (iii – v)). From the results, shifts in the characteristic Keggin peaks indicate the strong interaction between the MVP with DMDOA and the intactness of the Keggin structure. The resulting FTIR spectrum confirms that the ionic exchange reaction used in the formation of SEHs has no detrimental influence on the structure of the components.

The components of the as-prepared SEHs were determined using the thermo-gravimetric analysis. Minor weight loss below 100°C was observed due to the evaporation of water present within the interstitial of MLNS. As indicated in Fig. 5(d), the weight loss of the SEH–1, SEH–2 and SEH–3 are 58.4, 60.5 and 65.9% respectively. This indicates that the quaternary ammonium cations of DMDOA have fully replaced the protons of the HPA during the encapsulation process. The material is stable up to 200°C, after which the weight loss can be ascribed to the thermal decomposition of DMDOA ions. The good stability of DMDOA and the electrostatic based interaction with the MVP gives the SEHs increased stability as compared to POMs grafted with organic components.

3.2. Catalytic wet air oxidation performance evaluation

Fig. 6(a) shows the catalytic degradation of BPA with MVPA–2, SEH–1, SEH–2 and SEH–3 as the catalyst. Studies are carried out to understand the observed difference in catalytic activity, the possible mechanism and the stability of the SEHs. The deliberate design of the catalyst with hydrophobic properties inherited from the use of DMDOA acts as a molecular trap for the BPA molecules; this facilitates the redox interaction of the BPA with the catalytic MVP centre. During the catalytic reaction, the vanadium sites are the active sites for catalytic redox process.[29] The V^{5+} is reduced to V^{4+}, then re-oxidation of the V^{4+} site to V^{5+} is facilitated by the dissolved molecular oxygen species.[20, 30] The removal of BPA is higher in SEH–2 and SEH–3 as compared to SEH–1 over 180 min, primarily due to the higher degree of substitution of Mo by V.

Fig 6(b) shows the enhanced BPA removal under catalytic wet air oxidation. The concentration of dissolved oxygen species is maintained via interfacial reaeration, leading to an overall improvement in the removal of BPA. Since BPA is relatively non-volatile compound, aeration alone will be ineffective on

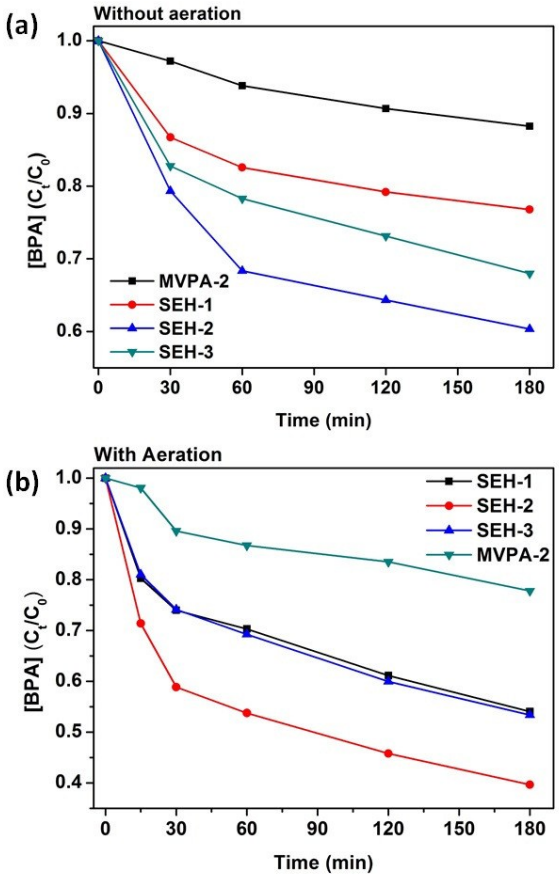

Fig. 6. (a) Removal efficiency of BPA using SEHs and MVPA–2 without aeration. (b) Removal efficiency of BPA using SEHs and MVPA–2 with aeration.

its removal. The enhancement in removal of BPA by SEH–1, SEH–2 and SEH–3 after the introduction of aeration is prominent. MVP–2 and MVP–3 incorporated into the SEHs are catalytic centres with capability to accept at least 2 electrons. This is due to the presence of at least 2 V^{5+} in the MVPAs incorporated, making re-oxidation by oxygen more favourable. As oxygen is a poor one-electron acceptor, re-oxidation is relatively unfavourable for the catalytic centres in SEH–1 (i.e. MVP–1) by oxygen due to the catalytic centre being a one-electron reduced species. While SEH–3 with 3 V^{5+} per active site should have higher catalytic performance than that of SEH–2, the inherent structural instability caused by the greater degree of substitution of molybdenum by vanadium[31] lead to SEH–2 out-performing SEH–3. Moreover, with the steric crowding of the surfactant around the catalytic site in SEH–3, it can also lead to reduced mass transport of BPA and radical species to and fro the active site and thus hinders the catalytic performance. Despite the specific surface area of SEH–2 being the lowest (1.46 m^2 g^{-1}) of the 3 SEHs prepared, it is shown that stability in combination with the nano-structure are important for the effective utilization of the material. The concentration of Mo^{6+} in solution is found to be approximately 0.002 % for all SEHs and severe leaching of 1.75% and 0.98% of V^{5+} was found for SEH–1 and SEH–3. The SEH–2 shows

exceptional stability with V^{5+} approximately 0.013% of leaching detected, which shows that the more efficient performance of SEH–2 was not due to effects of the active ions leaching into the solution. The influence of DMDOA to MVPA–2 ratio and solvent polarity on the catalytic activity of the materials prepared has also been studied (Fig. S1) showing that increase in surfactant stabilises and enhances the properties of MVP–2 to be a more effective catalyst. The lack of regularly formed MLNS within the material results in the poorer activity of the SEH–2 building blocks prepared without solvent polarity control. The increase in surfactant ratio also stabilizes MVPA–2 within the surfactant matrix, with vanadium leaching at 0.8% (i.e. when DMDOA : MVPA–2 is 2:1) to 0.1% in the building blocks (i.e. when DMDOA : MVPA–2 is 5:1).

To demonstrate that SEHs are superior to their unmodified counterpart, MVPA–2 corresponding to the mass fraction in SEH–2 (i.e. as determined from TGA) was used as a homogeneous catalyst for the removal of BPA. It can be seen from Fig. 6(a) and Fig. 6(b) that MVPA–2 is unable to effectively remove BPA as its use as a homogeneous catalyst requires careful control at ~pH 2 in order to prevent the hydrolysis of the Keggin anion at higher pH. Comparing this result with that obtained using SEH–2 shows that the surfactant modification has provided the desired enhancement in stability, efficiency and heterogeneity.

As the DMDOA surfactants make up a large percentage of SEHs composition as shown by TGA analysis, the plausibility of the BPA adsorption by SEHs has to be investigated. A control study with SEH–2 was employed for further investigation. The BPA solution was purged with argon for 30 min prior to catalytic testing. Fig. S2 shows the difference when oxygen is precluded from the solution. No significant contribution by adsorption is observed and only a slight drop in BPA concentration is detected after one hour, which is likely caused by small fraction of oxidation by the catalyst. The oxidative catalytic process was hindered due to lack of oxygen as a co-factor to interact with the catalytic centre for regeneration of active sites. Therefore, the effectiveness of the wet air oxidation process is dependent on the presence of dissolved oxygen.

Typical wet air oxidation processes operate through a free radical mechanism[32] which can be described by the following equations:

$$\mathrm{SEH} + \mathrm{n\,RH} \rightarrow \mathrm{SEH^{Red}} + \mathrm{n\,R\cdot} + \mathrm{n\,H^+} \quad (1)$$

$$\mathrm{R\cdot} + \mathrm{O_2} \rightarrow \mathrm{RO_2\cdot} \quad (2)$$

$$\mathrm{RO_2\cdot} + \mathrm{RH} \rightarrow \mathrm{ROOH} + \mathrm{R\cdot} \quad (3)$$

$$\mathrm{ROOH} \rightarrow \mathrm{RO\cdot} + \mathrm{\cdot OH} \quad (4)$$

where RH is the organic species and SEH^{Red} is the reduced SEH species; and the degradation of BPA via direct redox reaction centred on the SEH can be delineated by the following equations[33]:

$$\mathrm{SEH} + \mathrm{Red} \rightarrow \mathrm{SEH^{Red}} + \mathrm{Ox} \quad (5)$$

$$\mathrm{SEH^{Red}} + \tfrac{\mathrm{n}}{4}\mathrm{O_2} + \mathrm{nH^+} \rightarrow \mathrm{SEH} + \tfrac{\mathrm{n}}{2}\mathrm{H_2O} \quad (6)$$

where Red is the BPA and Ox is the oxidised BPA.

The MVP in SEH becomes reduced when mixed with the solution containing the organic pollutant as shown in Eq. (1). At pH 3 as shown in Fig. 7(a), the degradation of BPA is reduced as compared to natural pH conditions. The lower pH might reduce the formation of R^- by impeding the formation of R· in Eq. (1). At pH 9, the formation of R^- is more favourable, encouraging the propagation towards the generation of ·OH radical via free radical chain auto-oxidation process. This leads to an increase in the removal of BPA. However, we find that under natural pH condition (i.e. pH≈6.2), the removal of BPA is higher. The higher pH increases the formation of radical species; it may also counteract and adversely affect the re-oxidation of SEH in Eq. (6). Therefore, natural pH condition proves to be more favourable for the removal of BPA.

Reaction (2) and (3) are key processes in the production of ·OH radical. Therefore the regeneration of active sites on the SEH with aeration (Eq. (2)) to the solution can expedite the

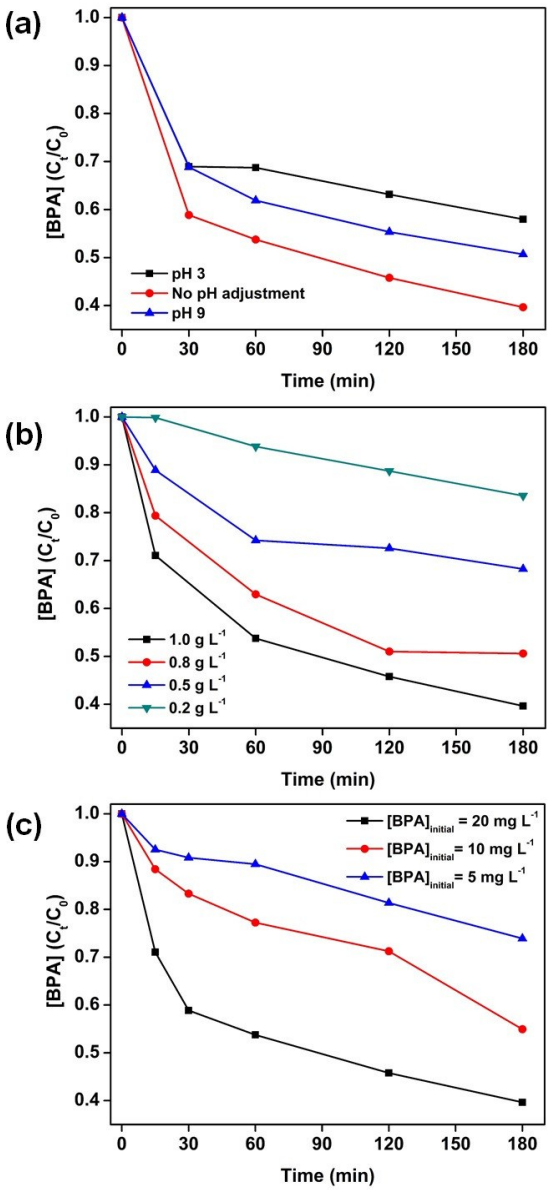

Figure 7. BPA removal efficiency (a) at pH3, pH9 and without pH adjustment; (b) at different SEH loading of 1.0, 0.8, 0.5, 0.2 g L^{-1} and (c) at initial BPA concentration of 20, 10, 5 mg L^{-1}.

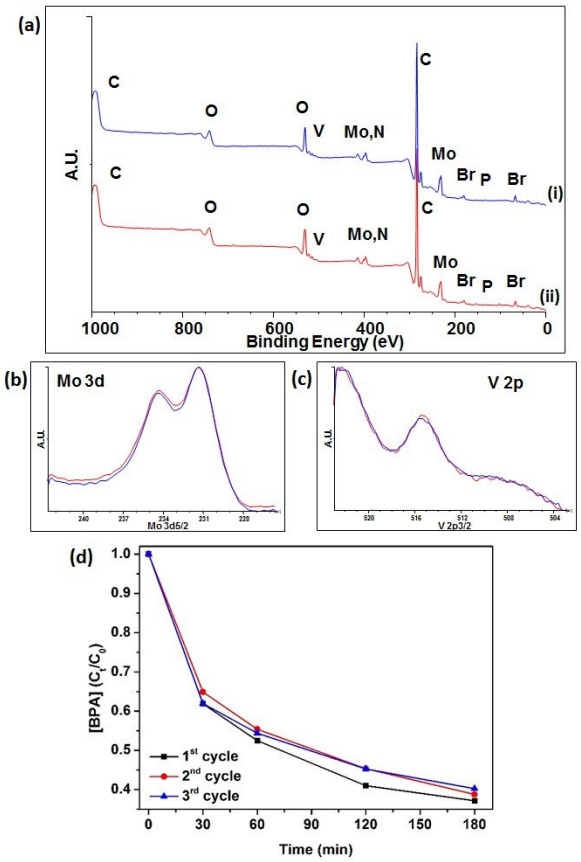

Fig. 8 XPS analysis results of SEH-2 (a) (i) before catalytic experiment and ii) after catalytic experiment. XPS spectra of (b) Mo and (c) V (blue = before catalytic experiment, red = after catalytic experiment). (d) BPA removal by SEH-2 over 3 consecutive cycles.

generation of ·OH (Eq. (4)) via autocatalytic decomposition and provide enhancement in the degradation efficiency of BPA. The lipophilic portion of the SEH will allow Red accompanied by oxygen to come into proximity with the active site of more easily. The consequent reduction of the MVP active site within the SEH is accompanied by the electron donor (i.e. BPA) being oxidised as outlined in Eq. (5). Oxygen is then responsible for oxidising the reduced POM site in SEH^{Red} in Eq. (6), mediating the redox process between V^{5+} and V^{4+} under mild conditions. This is evident from Fig. 6 where the removal of BPA is improved with the introduction of aeration to the system. The aeration also improves the re-oxidation of the SEH in Eq. 6, thereby giving enhancement in performance.

Fig. 7(b) presents the effects of SEH–2 loading on the removal of BPA. The removal of BPA was found to improve with the increase in SEH–2 loading. The increase in catalytic sites improves the reaction rate in Eq. (1) and (5) giving improvement in removal. Fig. 7(c) illustrates the influence of initial BPA concentration on the removal of BPA. The lower BPA concentration results in lower availability of BPA for the formation of R·. There is a lower production of ·OH which reduces the removal of BPA as a result.

In addition, XPS analysis was carried out on SEH–2 for evaluation of the practicality of regeneration of the catalyst (Fig. 8). Results from the analysis indicate that the catalyst structure is unaffected after use as there is little difference in the respective spectra of Mo 3d and V 2p (Fig. 8(b) and (c)) after reaction. The bromine found in the catalyst could be trapped within the MLNS during catalyst preparation and could have reduced the catalytic efficiencies of the SEHs as a radical scavenger. Fig. S3 shows the comparison of the FTIR spectrum of SEH–2 before and after catalytic application, we can see that the main difference is the loss of the broad OH stretching at ~3500 cm^{-1}. This is attributed to water trapped within the fresh catalyst during synthesis; while the catalyst was dried extensively post catalytic testing, leading to loss of the OH stretching peak. Moreover, we note that that characteristic peaks of MVP–2 and the surfactant component remains consistent between the two spectrum, indicating the stability of the catalyst and that BPA was not adsorbed on the SEH.

In comparison with previous work preparing amphiphiles comprising of POMs and surfactant which forms micellar catalyst within the solution,[34] the employment of a di-alkyl surfactant provides controllability in the formation of SEHs with MLNS. The encapsulation by surfactant allows the MVPs to be stabilised in a heterogeneous form within the SEH with 0.013% leaching of active vanadium species. This also provides a better platform for understanding of molecular ion catalysis in aqueous solutions. The SEHs being heterogeneous in an aqueous environment is another advantage of this material, as they could be recovered by simple filtration or centrifugation at the end of a catalytic process. Fig. 8(d) shows the recycling performance of SEH–2 over 3 cycles. SEH–2 is able to retain consistent level of BPA removal without a significant drop in performance (< 5%). This shows that the catalyst is relatively stable and can be effectively recycled after each catalytic reaction.

4. Conclusions

Nano-spherical surfactant encapsulated heteropolyanion for catalytic application were prepared with amphiphilic surfactant of DMDOA·Br and molybdovanadophosphoric acids as precursors for modification. The increment of anionic charge on the MVPAs has no significant influence on the morphology of the SEHs due to lower freedom of surfactant orientation around the POM. The selection of mixed solvent system of chloroform and *n*-butanol stabilises the particle size of the primary building blocks to be reduced towards the nano-sized dimension and isolated in stabilised dried state with controlled morphology. The current study has shown the promising potential of SEHs as an advanced functional material for catalytic wet air oxidation of organic pollutant under mild condition which is desirable as this reduces the related energy used and treatment cost. Although the surfactant increases the interaction probability of the target organic pollutant with the MVP catalytic centres, the catalytic efficiency of the system might also be reduced due to hindrance to mass transport of radical species for the propagation of degradation reaction throughout the system. While maintaining the advantages of stability and use of mild conditions in current

system, future research will look into (i) use of ionic-liquids with functionalised hydrophobic structure for added functionalities and (ii) strategies to improve the performance of the system by structural and morphological controls.

Acknowledgements

The author thanks Interdisciplinary Graduate School (IGS) and Nanyang Technological University for the award of research scholarship. We are grateful to Mr. Shima Masahide from JEOL, Japan for the XPS analysis performed. This work was supported by MOE Academic Research Fund (AcRF) Tier 1 RG 76/12 (M4011088.070).

Notes and references

1. Proust, A.; Thouvenot, R.; Gouzerh, P. *Chem Commun (Camb)* **2008**, (16), 1837-52.
2. Nisar, A.; Zhuang, J.; Wang, X. *Chemistry of Materials* **2009,** 21, (16), 3745-3751.
3. Omwoma, S.; Gore, C. T.; Ji, Y.; Hu, C.; Song, Y.-F. *Coordination Chemistry Reviews* **2015,** 286, 17-29.
4. Zhao, M.; Ou, S.; Wu, C.-D. *Accounts of Chemical Research* **2014,** 47, (4), 1199-1207.
5. Yanagie, H.; Ogata, A.; Mitsui, S.; Hisa, T.; Yamase, T.; Eriguchi, M. *Biomedicine & Pharmacotherapy* **2006,** 60, (7), 349-352.
6. Ji, Y.; Huang, L.; Hu, J.; Streb, C.; Song, Y.-F. *Energy & Environmental Science* **2015,** 8, (3), 776-789.
7. Lin, C. J.; Wang, S. L.; Huang, P. M.; Tzou, Y. M.; Liu, J. C.; Chen, C. C.; Chen, J. H.; Lin, C. *Water research* **2009,** 43, (20), 5015-5022.
8. Hiskia, A.; Mylonas, A.; Papaconstantinou, E. *Chemical Society reviews* **2001,** 30, (1), 62-69.
9. Hill, C. L. *Journal of Molecular Catalysis A: Chemical* **2007,** 262, (1-2), 2-6.
10. Hill, C. L.; Prossermccartha, C. M. *Coordination Chemistry Reviews* **1995,** 143, 407-455.
11. Wang, S.-S.; Yang, G.-Y. *Chemical Reviews* **2015,** 115, (11), 4893-4962.
12. Troupis, A.; Triantis, T. M.; Gkika, E.; Hiskia, A.; Papaconstantinou, E. *Applied Catalysis B: Environmental* **2009,** 86, (1-2), 98-107.
13. Mylonas, A.; Hiskia, A.; Papaconstantinou, E. *Journal of Molecular Catalysis a-Chemical* **1996,** 114, (1-3), 191-200.
14. Antonaraki, S.; Androulaki, E.; Dimotikali, D.; Hiskia, A.; Papaconstantinou, E. *Journal of Photochemistry and Photobiology a-Chemistry* **2002,** 148, (1-3), 191-197.
15. Misono, M. *Chemical communications* **2001**, (13), 1141-1152.
16. Nisar, A.; Wang, X. *Dalton Transactions* **2012,** 41, (33), 9832-9845.
17. Mirzaei, M.; Eshtiagh-Hosseini, H.; Alipour, M.; Frontera, A. *Coordination Chemistry Reviews* **2014,** 275, 1-18.
18. Liu, S.; Tang, Z. *Nano Today* **2010,** 5, (4), 267-281.
19. Long, D. L.; Tsunashima, R.; Cronin, L. *Angewandte Chemie-International Edition* **2010,** 49, (10), 1736-1758.
20. Neumann, R.; Khenkin, A. M. *Chemical communications* **2006**, (24), 2529-2538.
21. Khenkin, A. M.; Neumann, R. *Chemsuschem* **2011,** 4, (3), 346-348.
22. Ettedgui, J.; Neumann, R. *Journal of the American Chemical Society* **2009,** 131, (1), 4.
23. Zubrzycki, R.; Epping, J. D.; Ressler, T. *ChemCatChem* **2015,** 7, (7), 1112-1121.
24. Kim, K. H.; Ihm, S. K. *Journal of Hazardous Materials* **2011,** 186, (1), 16-34.
25. Tsigdino.Ga; Hallada, C. J. *Inorganic Chemistry* **1968,** 7, (3), 437-&.
26. Nisar, A.; Xu, X.; Shen, S.; Hu, S.; Wang, X. *Advanced Functional Materials* **2009,** 19, (6), 860-865.
27. Rocchiccioli-Deltcheff, C.; Fournier, M.; Franck, R.; Thouvenot, R. *Inorganic Chemistry* **1983,** 22, (2), 207-216.
28. Okuyama, K.; Soboi, Y.; Iijima, N.; Hirabayashi, K.; Kunitake, T.; Kajiyama, T. *Bulletin of the Chemical Society of Japan* **1988,** 61, (5), 1485-1490.
29. Molinari, J. E.; Nakka, L.; Kim, T.; Wachs, I. E. *ACS Catalysis* **2011,** 1, (11), 1536-1548.
30. Ressler, T.; Timpe, O.; Girgsdies, F.; Wienold, J.; Neisius, T. *Journal of Catalysis* **2005,** 231, (2), 279-291.
31. Neumann, R. *Inorganic Chemistry* **2010,** 49, (8), 3594-3601.
32. Zhang, Y.; Li, D. L.; Chen, Y.; Wang, X. H.; Wang, S. T. *Applied Catalysis B-Environmental* **2009,** 86, (3-4), 182-189.
33. Kozhevnikov, I., *Catalysts for Fine Chemical Synthesis, Catalysis by Polyoxometalates*. Wiley: 2002.
34. Zhao, S.; Wang, X.; Huo, M. *Applied Catalysis B: Environmental* **2010,** 97, (1–2), 127-134.